Experimental Study of the Reaction between Vinyl and Methyl Radicals in the Gas Phase. Temperature and Pressure Dependence of Overall Rate Constants and Product Yields

Stanislav I. Stoliarov,[†] Vadim D. Knyazev,[†,‡] and Irene R. Slagle*[,†]

Department of Chemistry, The Catholic University of America, Washington, D.C. 20064, and Physical and Chemical Properties Division, National Institute of Standards and Technology, Gaithersburg, Maryland 20899-8380

Received: July 20, 1999; In Final Form: April 5, 2000

The vinyl−methyl cross-radical reaction was studied by laser photolysis/photoionization mass spectroscopy. Overall rate constants and quantitative product yields were obtained in direct real-time experiments in the temperature region 300−900 K and bath gas (He) density (3−12) × 10^{16} molecules cm^{-3}. The observed overall $C_2H_3 + CH_3$ rate constant is independent of pressure and demonstrates a slight negative temperature dependence, which can be represented by the expression $k_4 = 5.1 \times 10^{-7}T^{-1.26}$ exp(−362/T) $molecule^{-1}$ cm^3 s^{-1} (The expression has ±10% uncertainty, see text for details.). Propene, acetylene, and allyl radicals were identified as primary products of the $C_2H_3 + CH_3$ reaction. At room temperature propene and acetylene are the major products of the reaction, whereas at 900 K production of allyl radicals becomes the dominating channel. On the basis of these experimental results, a mechanism consisting of two major routes is proposed. One route proceeds via direct abstraction of a hydrogen atom from the vinyl radical by the methyl radical resulting in the formation of acetylene and methane. The other route proceeds via the formation of chemically activated propene that can undergo either collisional stabilization or further decomposition into allyl radical and hydrogen atom.

I. Introduction

Radical−radical cross-combination reactions constitute an integral part of the overall mechanisms of oxidation and pyrolysis of hydrocarbons.[1,2] Reliable rate and branching data on this type of reactions are sparse as they are difficult to study experimentally due to the high reactivity of the chemical species involved. Recombination reactions involving alkyl radicals lead to formation of stable species and serve as termination processes in the combustion environment. At the same time, similar reactions involving unsaturated radicals can possess more complex mechanisms that include chemically activated channels of further decomposition of the vibrationally excited adduct formed in the initial addition step. Such reactions are characterized by complex temperature and pressure dependencies of the overall rate constants and branching channel ratios.

The reaction between vinyl and methyl radicals is the simplest of the class of reactions between alkenyl and alkyl radicals. This reaction plays an important role in mechanisms of evolution of planetary atmospheres.[3,4] Methyl and vinyl radicals are also critical intermediates in hydrocarbon combustion systems with elementary reactions of CH_3 and C_2H_3 influencing the rate and products of the overall combustion process.[2]

Very little experimental information is available on the $C_2H_3 + CH_3$ reaction. Fahr et al.[5] determined the rate constants of two reaction channels at room temperature and 13.3 kPa (100 Torr) of He using laser photolysis−kinetic UV absorption spectroscopy:

$$C_2H_3 + CH_3 \rightarrow CH_2CHCH_3 \qquad k = (1.2 \pm 0.3) \times 10^{-10}\ \text{molecule}^{-1}\ \text{cm}^3\ \text{s}^{-1}$$

$$\rightarrow CH_4 + C_2H_2 \qquad k = (0.34 \pm 0.07) \times 10^{-10}\ \text{molecule}^{-1}\ \text{cm}^3\ \text{s}^{-1}$$

The rate constants were derived from monitoring the real-time kinetics of CH_3 decay and C_4H_6 formation, end-product analysis, and detailed modeling of the kinetic mechanism.

Here we present the results[6] of a direct experimental investigation of the vinyl−methyl cross-radical reaction by means of laser flash photolysis/time-resolved photoionization mass spectrometry. Overall rate constants and product yields were obtained in the temperature region 300−900 K and bath gas (He) density (3−12) × 10^{16} molecules cm^{-3}.

II. Experimental Setup

Details of the experimental apparatus have been described previously.[7,8] Only a brief description is presented here. Pulsed 193-nm unfocused collimated radiation from a Lambda Physik 201 MSC[9] ArF excimer laser was directed along the axis of a 50-cm-long 1.0-cm-i.d. heatable tubular quartz reactor. The intensity of the radiation was uniform (<5% deviation) along the 20-cm zone of the reactor that was used for the kinetic measurements. The laser was operated at 4 Hz and at a fluence of 100−180 mJ/pulse. The energy flux of the laser radiation inside the reactor was in the range of 1−40 mJ/cm^2 per pulse depending on the degree of laser beam attenuation.

Gas flowing through the tube at ≈4 m s^{-1} (to replace the photolyzed gas with a fresh reactant gas mixture between the laser pulses) contained free radical precursors in low concentrations and the bath gas, helium. The gas was continuously sampled through a 0.04-cm-diameter tapered hole in the wall

[†] The Catholic University of America.
[‡] National Institute of Standards and Technology.

10.1021/jp992476e CCC: $19.00
Published on Web 10/05/2000

of the reactor (gas-sampling orifice) and formed into a beam by a conical skimmer before it entered the vacuum chamber containing the photoionization mass spectrometer (PIMS). The pressure in the chamber was kept below 1.3×10^{-3} Pa (1×10^{-5} Torr). As the gas beam traversed the ion source, a portion was photoionized using an atomic resonance lamp,[10] mass selected in an EXTREL[9] quadrupole mass filter, and detected by a Daly[11] detector. A hydrogen resonance lamp with MgF_2 window was used to monitor molecules with ionization potential (IP) below the energy of the Lyman α line, 10.2 eV ($CH_3C(O)CH_3$, $C_2H_3C(O)CH_3$, C_2H_3Br, CH_3CO, C_2H_2CO, C_2H_3, CH_3, C_3H_6, C_3H_5, C_4H_8, C_3H_4 (allene or cyclopropene)). An argon resonance lamp (11.6, 11.8 eV) with LiF window was used for the molecules with IP > 10.2 eV (CH_2, C_2H_2, C_2H_4, C_3H_4 (propyne)). Both lamps were employed for detection of molecules with unknown ionization potentials. The near threshold ionization conditions provided by the resonance lamps allowed all species to be monitored at the mass-to-charge ratio (m/z) of the corresponding parent ions.

Temporal ion signal profiles were recorded from 10−30 ms before each laser pulse to 15−35 ms following the pulse by using an EG&G ORTEC[9] multichannel scaler interfaced with a PC computer. Typically, data from 500 to 25 000 repetitions of the experiment were accumulated before the data were analyzed.

The tubular reactor was heated by passing a direct current through a 1-cm-wide Nichrome ribbon tightly wrapped around the reactor in a spiral that extends from 20 cm upstream to 15 cm downstream from the sampling orifice. The temperature during the experiments was monitored by a thin (1/16-in. o.d.) in situ thermocouple placed in the heated zone of the reactor 2.5 cm downstream from the sampling orifice. The temperature profiles along the axis of the reactor were recorded with a movable thermocouple placed further upstream for each set of experimental conditions used. The temperature readings of the movable thermocouple were in good agreement (±4 K at 500 K, ±7 K at 900 K) with the temperature reading of the stationary thermocouple used to monitor temperature during the rate constant and product yield measurements.

The reactor was operated in the temperature region 300−900 K and helium bath gas density $(3-12) \times 10^{16}$ molecules cm^{-3}. The pressure was measured through a reactant inlet 30 cm upstream from the sampling orifice and corrected for an axial viscous pressure drop[12] in order to determine the pressure in the middle of the reaction zone (approximately 8 cm upstream from the sampling orifice). The correction never exceeded 5% of the measured pressure value. The operating conditions assume a plug flow regime[13] for the gas flowing through the reactor. Under these conditions, the radial temperature profile is flat. Small radial variations of the initial concentrations of species produced in the photolysis (which are due to the radial variations of laser intensity) are rapidly removed by diffusion ($\tau < 2$ ms).

The flow system was regularly checked for air leaks by measuring a pressure increase over time. During these measurements, a portion of the reactor inside the mass spectrometer high-vacuum chamber was replaced by a plug. Pressure was measured with an MKS122A00010AD capacitance manometer (MKS Instruments).[9] A typical pressure buildup of less than 5 mTorr over a period of 30 min in a volume of 368 cm^3, combined with the He flow parameters listed above, translates into an upper limit of 10^{11} molecules cm^{-3} for the concentration of air in the reactor.

The inside of the tubular quartz reactor was periodically cleaned with a 5% $NH_4F{\cdot}HF$ aqueous solution and coated with a 5% boric acid aqueous solution, which was subsequently transformed to boron oxide by heating the reactor to 900 K.[14] This procedure was performed in order to minimize heterogeneous free radical wall-loss processes (See section IV, subsection "Procedure", for a more detailed description of heterogeneous processes.). In addition, an uncoated quartz reactor was used in the overall rate constant measurement part of this work in order to test the effects of wall conditions on the kinetics of the reaction.

Materials. Acetone (>99.9%), acetone-d_6 (100.0% D), methyl vinyl ketone (99.0%), vinyl bromide (98.0%), allyl bromide (99.0%), 1,5-hexadiene (97.0%), ethylene (>99.5%), propene (>99.0%), and 1-butene (>99.0%) were obtained from Aldrich[9] and purified by vacuum distillation prior to use. Acetone-*2*-^{13}C (99% 2-^{13}C) was obtained from Cambridge Isotope Laboratories[9] and used as provided. Helium (>99.999%, $[O_2] < 1.5$ ppm, MG Industries[9]) and argon (>99.99%, Matheson[9]) were used without further purification.

III. Photolysis of Precursors

The photolysis of acetone at 193 nm, which was used in this study as a source of methyl radicals, was shown by Lightfoot et al.[15] to proceed predominantly (>95%) via channel 1a under

$$CH_3C(O)CH_3 \xrightarrow{193\ nm} 2CH_3 + CO \quad (1a)$$

$$\rightarrow H + CH_2C(O)CH_3 \quad (1b)$$

$$\rightarrow CH_4 + CH_2CO \quad (1c)$$

conditions similar to those used in the current work. Reactions 1b and 1c were determined to occur to a minor degree, <3% and <2%, respectively.

The 193-nm photolysis of methyl vinyl ketone, used in this work as a precursor for vinyl radicals, was shown by Fahr et al.[16] to occur via reaction 2 (∼100%) at room temperature and 13.3 kPa (100 Torr) of He.

$$C_2H_3C(O)CH_3 \xrightarrow{193\ nm} CH_3 + C_2H_3 + CO \quad (2)$$

An analysis of the 193-nm photolysis of $C_2H_3C(O)CH_3$ at 300 and 900 K ($[He] = 3 \times 10^{16}$ and 12×10^{16} molecules cm^{-3}) has been conducted in the current work. In addition to channel 2 the only observed products attributed to the photolysis of methyl vinyl ketone were CH_3CO (m/z 43), C_2H_2CO (m/z 54), and CH_2 (m/z 14). The signal intensities of these products were close to the sensitivity limit of the equipment. Weak signals at m/z 26 (C_2H_2), 28 (C_2H_4), and 42 (CH_2CO or C_3H_6) were also observed. These products could either come directly from the $C_2H_3C(O)CH_3$ photolysis or be produced in $C_2H_3 + CH_3$ or $C_2H_3 + C_2H_3$ secondary reactions. The signals were too weak to establish the origins of these products.

The 193-nm photolysis of vinyl bromide was used as an alternative source for vinyl radicals. The photolysis was studied previously by Slagle et al.[8] within a range of experimental conditions similar to those used in this investigation. The only two significant routes that were detected were reaction 3a (≈43%) and 3b (≈57%).

$$C_2H_3Br \xrightarrow{193\ nm} C_2H_3 + Br \quad (3a)$$

$$\rightarrow C_2H_2 + HBr \quad (3b)$$

IV. Determination of the Overall $C_2H_3 + CH_3$ Rate Constant

Method. CH_3 and C_2H_3 radicals were produced simultaneously by the 193-nm photolysis of a mixture of corresponding

precursors (acetone for CH_3 and methyl vinyl ketone or vinyl bromide for C_2H_3) highly diluted in the helium carrier gas (>99%). The $C_2H_3 + CH_3$ rate constant measurements were performed using a technique analogous to that applied by Niiranen and Gutman to the studies of the $SiH_3 + CH_3$ and $Si(CH_3)_3 + CH_3$ kinetics,[17] which is a further development of the method used by Garland and Bayes to study a series of radical cross-combination reactions.[18] Experimental conditions (in particular, the two precursor concentrations) were selected to create a large excess of initial concentrations of methyl radicals over the total combined concentration of all the remaining radicals formed in the system. The initial concentration of methyl radicals was typically 20−80 times higher than that of C_2H_3. Under these conditions, the self-recombination of methyl radicals was essentially unperturbed by the presence of the other radicals. At the same time, the kinetics of C_2H_3 was completely determined by the reaction with CH_3 and unaffected either by self-recombination or by reactions with other active species formed in the system (including the products of the $C_2H_3 + CH_3$ reaction).

The reactions of C_2H_3 and CH_3 with acetone (the precursor of methyl radicals) did not have to be taken into account due to their negligible rates. The upper limit of the rate constant of the reaction between CH_3 and $CH_3C(O)CH_3$, within the range of experimental conditions used, is approximately 3×10^{-15} molecule^{-1} cm^3 s^{-1}.[19] The reaction of C_2H_3 with acetone can be expected to be of the same order of magnitude. The effects of reactions of C_2H_3 and CH_3 radicals with the vinyl radical precursors ($C_2H_3C(O)CH_3$ or C_2H_3Br) could be neglected due to the negligible rates and low concentrations of the precursors. The concentrations of the vinyl radical precursors used in these experiments were approximately 2 orders of magnitude lower than that of acetone.

Heterogeneous loss was the only additional sink of methyl and vinyl radicals that had to be taken into account (See subsection "Procedure" for details.). Thus, the kinetic mechanism of the important loss processes of methyl and vinyl radical in these experiments is as follows:

$$C_2H_3 + CH_3 \rightarrow \text{products} \quad (4)$$

$$CH_3 + CH_3 \rightarrow C_2H_6 \quad (5)$$

$$C_2H_3 \rightarrow \text{heterogeneous loss} \quad (6)$$

$$CH_3 \rightarrow \text{heterogeneous loss} \quad (7)$$

For this mechanism and for the initial conditions described above, the system of first-order differential equations can be solved analytically.

$$\frac{CH_3^+\ \text{signal}_t}{CH_3^+\ \text{signal}_0} = \frac{[CH_3]_t}{[CH_3]_o} = \frac{k_7 \exp(-k_7 t)}{2k_5[CH_3]_0\,(1 - \exp(-k_7 t)) + k_7} \quad \text{(I)}$$

$$\frac{C_2H_3^+\ \text{signal}_t}{C_2H_3^+\ \text{signal}_0} = \frac{[C_2H_3]_t}{[C_2H_3]_0} = \exp(-k_6 t)\left[\frac{k_7}{2k_5[CH_3]_0(1 - \exp(-k_7 t)) + k_7}\right]^{k_4/2k_5} \quad \text{(II)}$$

These analytical solutions (eqs I and II) were used to fit experimental signal profiles in order to obtain the rate constants of interest, k_4 and k_5. The essential feature of this method is that the exact knowledge of the initial concentration of vinyl radicals is not required for the determination of the rate constants. In this respect, the approach is similar to the pseudo-first-order method frequently applied to studies of kinetics of second-order reactions.

Procedure. The first-order decay ($k = 2-60$ s^{-1}) of vinyl or methyl radicals was observed in experiments with no reactants other than the corresponding precursor present in the system, and the initial concentration of the radicals produced in the photolysis decreased to the point where the rates of radical combination reactions are negligible. The rate of the decay did not depend on the concentration of the precursor, laser intensity, or bath gas (He) density, but was affected by wall conditions of the reactor (such as coating and history of exposure to reactive mixtures). The decay was attributed to heterogeneous loss processes. The rate constants of heterogeneous loss of methyl (k_7) and vinyl (k_6) radicals were determined in separate sets of measurements. The reduction of the initial concentrations of the radicals was performed by attenuating the photolyzing laser beam with quartz plates and/or wire mesh until the rate constant of heterogeneous loss was independent of initial radical concentration. The signal profiles obtained were fitted with a first-order rate expression in order to determine the rate constant of heterogeneous loss.

The only potential bimolecular reactions that could augment the rate of decay of radicals in the absence of other reactants are those with molecular oxygen. However, the concentration of oxygen contaminant both from the small O_2 impurity in the helium and from potential leaks is negligibly small, less than 2×10^{11} molecules cm^{-3} under all experimental conditions (see above). Therefore, this potential contribution to radical decay would not exceed 2 s^{-1} in the case of vinyl radical[8] and 0.5 s^{-1} in the case of CH_3 radical.[1] These potential $R + O_2$ processes would manifest themselves as, at most, minor additions to the heterogeneous wall processes, which, in turn, are minor compared with the reaction under study (vide infra). Thus, these processes cannot influence the results of the rate constant and product yield measurements to any notable extent. The products of the $R + O_2$ reactions, if present at all, would not affect the observed kinetics due to their low concentrations.

The initial concentration of methyl radicals was determined by measuring the photolytic depletion of acetone. The value of the decomposition ratio (the relative decrease in the precursor concentration upon photolysis) was obtained directly from the acetone ion signal profile (A typical profile is shown in Figure 1.) and corrected for the ion signal background. The background was mainly due to a low constant concentration of precursor molecules (acetone, in this case) in the mass spectrometer chamber and the interaction of the scattered UV light from the resonance lamp with the high-voltage target of the Daly detector. The signal of the scattered light (usually 0.5−2% of the signal of the precursor) was measured at *m*/*z* 10 (There are no ions at this mass.) before and after each precursor decomposition measurement.

The part of background associated with the constant concentration of molecules in the mass spectrometer chamber originates from ionization of molecules that either are always in the vacuum chamber (e.g., oil vapors) or come from the reactor but are not photoionized as they pass through the ionization region; instead these neutral molecules collide with the walls or with other neutrals and eventually return to the ionization region where they are photoionized, mass selected, and detected. This part of the background does not adjust instantaneously to rapid changes of concentration of molecules in the reactor after

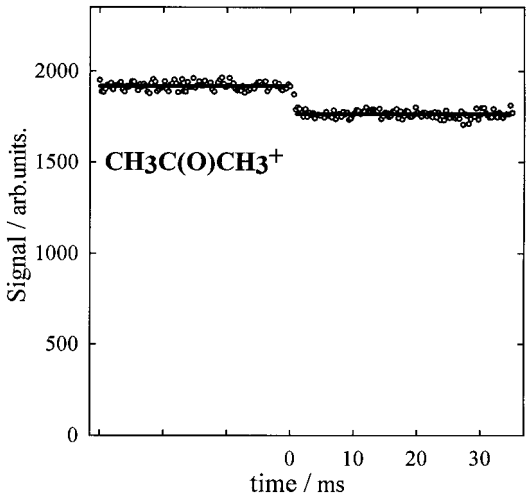

Figure 1. Acetone ion signal profile used to determine $[CH_3]_0$. T = 500 K, [He] = 6.0×10^{16} molecules cm^{-3}, $[CH_3C(O)CH_3]_0 = 4.5 \times 10^{13}$ molecules cm^{-3}. The straight horizontal lines are the average of the signals before and after the laser pulse. $DR(CH_3C(O)CH_3) = 0.095$.

the photolyzing laser pulse; it remains constant during the 20−40 ms period following the laser pulse. Although this steady-state-concentration part of the background has to be accounted for when measuring signals of stable molecules that are continuously present in the reactor (such as radical precursors), it does not contribute to the ion signals of free radicals since (1) these species are present in the reactor only during a very short time following the laser pulse and (2), being highly reactive, radicals cannot "survive" in the mass spectrometer chamber for any extended period of time.

The part of background associated with the steady-state concentration of the precursor molecules in the mass spectrometer chamber was determined in separate measurements (the photolyzing laser was turned off) by decreasing the pumping speed (thus increasing the pressure in the chamber) and measuring the increase in the signal of the precursor. The background part of the signal is proportional to the pressure in the chamber whereas the part of the signal that corresponds to molecules that come directly from the reactor is unaffected by the change in pumping speed. The background to background-plus-signal ratio ($B/(B + S)$) was determined from these measurements. The value of $B/(B + S)$ (typically, 0.05−0.15) varied slightly with the change in experimental conditions (T, [He]) and was stable during each set of experiments. The corrected decomposition ratio (DR) was obtained by using the expression

$$DR = \frac{\text{signal}_{\text{before laser pulse}} - \text{signal}_{\text{after laser pulse}}}{(\text{signal}_{\text{before laser pulse}} - \text{signal}_{\text{scattered light}})\left(1 - \frac{B}{B+S}\right)} \quad \text{(III)}$$

The background does not change after the laser pulse and, therefore, cancels out in the numerator of expression III. However, both contributions to the background had to be accounted for in the denominator.

The DR value of acetone varied from 0.06 to 0.17 depending on the experimental conditions (laser radiation fluence and temperature). The value of $[CH_3]_0$ was taken to be twice that of the measured depletion in the acetone concentration (2(DR)-$[CH_3C(O)CH_3]$). The minor acetone photolysis routes (1b and 1c) were taken into account only when C_2H_3Br was used as the precursor for vinyl radicals. In the case of methyl vinyl ketone as the precursor for C_2H_3, the small systematic overdetermination of $[CH_3]_0$ as a result of the neglect of the minor routes of acetone photolysis was largely canceled out, under the experimental conditions used, by disregarding the production of methyl radicals in the photolysis of $C_2H_3C(O)CH_3$. The initial concentration of vinyl radicals was estimated (no correction for $B/(B + S)$ was made) using the same approach as for methyl radicals ($DR(C_2H_3C(O)CH_3) \approx 0.2-0.5$, $DR(C_2H_3Br) \approx 0.2-0.4$). Reaction 2 was assumed to be the only route of photolysis of methyl vinyl ketone within the range of experimental conditions used. Branching in the vinyl bromide photolysis was taken into account.

The procedure of determination of the $C_2H_3 + CH_3$ rate constant for each set of experimental conditions consisted of the following sequence of measurements:

1. Kinetics of heterogeneous loss of C_2H_3 (determination of k_6). Only the vinyl radical precursor is in the system.

2. Kinetics of heterogeneous loss of CH_3 (determination of k_7). Only acetone is in the system.

3. Decomposition ratio of vinyl radical precursor (determination of $[C_2H_3]_0$). Both radical precursors are in the system.

4. Decomposition ratio of acetone (determination of $[CH_3]_0$). Both radical precursors are in the system.

5. Kinetics of methyl radicals in the presence of vinyl radicals (determination of k_5).

6. Kinetics of vinyl radicals in the presence of methyl radicals (determination of k_4).

Measurements 1−5 were repeated in reverse order (except for 3) after monitoring the kinetics of vinyl radicals in the presence of methyl radicals in order to ensure the stability of initial concentrations of CH_3 and the rate constants of heterogeneous loss (k_6 and k_7) during the time of the experiment. The $B/(B + S)$ of acetone was determined after each set of these measurements.

Results. Typical CH_3^+ and $C_2H_3^+$ decay profiles are shown in Figure 2. The lines through the CH_3^+ and $C_2H_3^+$ data points are from a fit with expressions I and II, respectively. CH_3^+ profiles were fitted using values of k_7 measured in step 2. $C_2H_3^+$ profiles were fitted using values of k_5, k_6, k_7, and $[CH_3]_0$ measured in steps 5, 1, 2, and 4, respectively. The first 2 ms of data following the laser pulse were not used in the fit of the signal profiles in order to ensure homogeneity of concentrations and full vibrational relaxation of the radicals formed in the photolysis of the precursors.[20] The zero time point was chosen to be at the half-height of the rising part of the radical signal and usually coincided for CH_3^+ and $C_2H_3^+$ profiles (typically, about 0.2 ms following the laser pulse).

The $C_2H_3 + CH_3$ rate constant measurements were performed within the following range of experimental conditions: T = 300−900 K, [He] = (3−12) $\times 10^{16}$ molecules cm^{-3}. The conditions and results of all experiments are presented in Table 1. The values of the $C_2H_3 + CH_3$ and $CH_3 + CH_3$ rate constants (k_4 and k_5 respectively) did not depend on $[CH_3]_0$ or $[C_2H_3]_0$, which were varied by approximately a factor of 2 (with temperature and bath gas density kept constant) by changing either the laser fluence or precursor concentration in order to test the veracity of the kinetic model. Heterogeneous loss was a minor channel of consumption of methyl and vinyl radicals with respect to the major channels, reaction 5 and reaction 4, respectively. The rate constants of heterogeneous loss of methyl (k_7) and vinyl (k_6) radicals depended on the quality of the boron oxide reactor wall coating, which, in turn, depended on the history of exposure to the reaction environment. k_6 increased sharply when an uncoated quartz reactor was used. k_4 and k_5

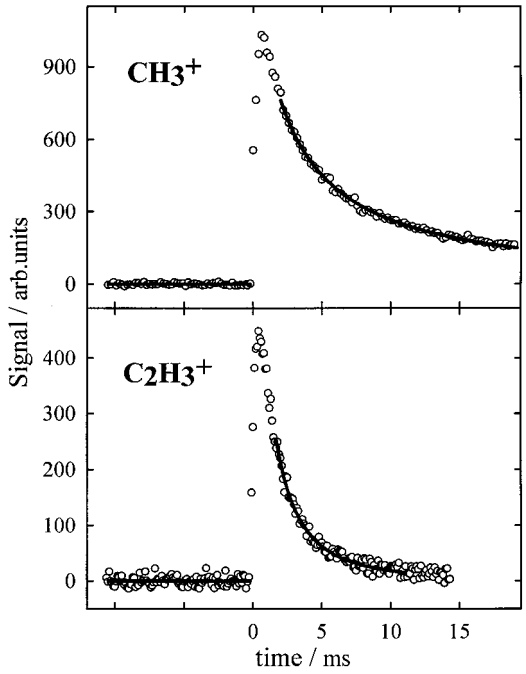

Figure 2. CH_3 and C_2H_3 ion signals recorded during one set of experiments to study the kinetics of the $C_2H_3 + CH_3$ reaction. T = 500 K, [He] = 6.0×10^{16} molecules cm^{-3}, $[CH_3]_0 = 8.6 \times 10^{12}$ molecules cm^{-3}, $[C_2H_3]_0 = 2.2 \times 10^{11}$ molecules cm^{-3}. Solid curves represent fitting of the experimental data with the corresponding rate constant expressions (I for CH_3 and II for C_2H_3). $k_5 = 2.3 \times 10^{-11}$ molecule^{-1} cm^3 s^{-1}, $k_4 = 1.08 \times 10^{-10}$ molecule^{-1} cm^3 s^{-1}.

were not affected by the reactor wall condition, indicating that potential heterogeneous effects had no influence on the reaction under study. The rate constants also did not depend on the nature of vinyl radical precursor. For several sets of experimental conditions used in this study (primarily those with the lower $[CH_3]_0/[C_2H_3]_0$) the CH_3^+ signal profile was monitored both in the presence and in the absence of the C_2H_3 precursor. These experiments verified that the CH_3 decay exhibited no change with the introduction of the C_2H_3 precursor, as expected due to the initial conditions used and the mechanism presumed.

Although the measurement of k_5 was not the goal of the current work, the experiments yielded some new rate constant information on the $CH_3 + CH_3$ reaction. The results obtained are in good agreement with those previously measured in this laboratory,[20] an additional indication of the fact that the presence of vinyl radical precursor in the system did not perturb the kinetics of methyl radicals to any detectable extent. The new results extend the pressure and temperature range of the previous measurements of k_5 in He bath gas (see Table 1).

An Arrhenius plot of the $C_2H_3 + CH_3$ rate constants (k_4) is shown in Figure 3 (The uncertainties are not shown on the plot to avoid congestion.). The observed rate constants decrease slightly with increasing temperature and show no pressure dependence within the range of experimental conditions. The parametric fit of the temperature dependence (solid line on the plot) is given by the expression

$$k_4 = 5.1 \times 10^{-7} T^{-1.26} \exp(-362/T) \text{ molecule}^{-1} \text{ cm}^3 \text{ s}^{-1} \quad \text{(IV)}$$

The expression has ±10% uncertainty (See Table 1 for uncertainties of data at individual temperatures and section VI for the methods of estimation of the uncertainties.). The statistical uncertainties of the fit (2σ) are as follows: $2\sigma(\log(A)) = 1.26$, $2\sigma(n) = 0.4$, $2\sigma(E) = 195$ K (if the rate constant is expressed as $k = AT^n \exp(-E/T)$). These values, however, refer to a parametrized fit and have no physical meaning.[27] The room-temperature rate constant values of the current study agree within the experimental uncertainty limits with that of Fahr et al.[5] (also presented in Figure 3).

V. Product Analysis of the $C_2H_3 + CH_3$ Reaction

The product analysis was performed within the same range of experimental conditions (T = 300−900 K, [He] = (3−12) × 10^{16} molecules cm^{-3}) as the overall rate constant measurements. $[CH_3]_0/[C_2H_3]_0$ was again kept high (>19) in order to ensure that the only important channel of consumption of vinyl radicals (besides the heterogeneous loss) was the reaction under study. In the product analysis only $C_2H_3C(O)CH_3$ was used as a precursor for vinyl radicals. The use of vinyl bromide was ruled out because the major route of photolysis (3b) produces C_2H_2, one of the potential products of the $C_2H_3 + CH_3$ reaction. Acetone-*2*-^{13}C was used as a precursor for methyl radicals instead of normal acetone. The use of the isotope-substituted reagent was dictated by the presence of a minor channel of the photolysis of acetone producing ketene (1c). Ketene (CH_2CO) has the same mass as another potential product of the $C_2H_3 + CH_3$ reaction, propene. These two species have nearly identical ionization potentials.[21] Although the photolysis yield of ketene is small (<2%), the absolute concentration produced under the experimental conditions used is comparable with $[C_2H_3]_0$. The substitution of normal acetone with $CH_3{}^{13}C(O)CH_3$ shifts the mass of the produced ketene ($CH_2{}^{13}CO$) up one mass unit (m/z 43) with respect to propene (m/z 42), thus allowing for clear detection of the potential product without any changes in the kinetic system under study. The 193-nm photolysis of $CH_3{}^{13}C(O)CH_3$ was presumed to have the same mechanism and product yields as that of $CH_3{}^{12}C(O)CH_3$.

Identification of Products. The $C_2H_3 + CH_3$ system was analyzed for the presence of the following products: C_3H_6 (propene or cyclopropane), C_2H_2 (acetylene), C_3H_4 (propyne, allene, or cyclopropene), C_3H_5 (allyl radical), C_2H_4 (ethylene), CH_2 (methylene). C_3H_6, C_3H_5, and C_2H_2 products were detected within the range of experimental conditions used. Ion signal profiles of these products obtained at 310 K and [He] = 12 × 10^{16} molecules cm^{-3} are shown in Figure 4. The detection of these products suggests the following channels of the $C_2H_3 + CH_3$ reaction:

$$C_2H_3 + CH_3 \rightarrow C_3H_6 \quad \text{(4a)}$$

$$\rightarrow C_3H_5 + H \quad \text{(4b)}$$

$$\rightarrow C_2H_2 + CH_4 \quad \text{(4c)}$$

In addition, formation of C_4H_8 was detected (Figure 4). The "rise time" of the C_4H_8 product signal was significantly longer than that of C_3H_6, C_2H_2, and C_3H_5 indicating that C_4H_8 is, most likely, produced in a secondary reaction. The formation of C_4H_8 was attributed to the reaction between allyl and methyl radicals:

$$C_3H_5 + CH_3 \rightarrow C_4H_8 \quad (8)$$

At the time of formation of C_3H_5, the methyl radicals are still in a large excess over the total concentration of all the remaining active species formed in the system. Therefore, reaction with methyl radicals (reaction 8) and heterogeneous loss of C_3H_5

$$C_3H_5 \rightarrow \text{heterogeneous loss} \quad (9)$$

TABLE 1: Experimental Conditions and Rate Constants Obtained in the Study of the $C_2H_3 + CH_3$ Reaction

10^{-16}[He], molecules cm^{-3}	T, K	10^{-11}[C_4H_6O]/10^{-13}[C_3H_6O], molecule cm^{-3}	10^{-11}[C_2H_3]$_0$/10^{-12}[CH_3]$_0$, molecule cm^{-3}	k_7, s^{-1}	k_6, s^{-1}	$10^{11}k_5$,[a] molecule^{-1} cm^3 s^{-1}	$10^{10}k_4$,[a,b] molecule^{-1} cm^3 s^{-1}
Room Temperature, $k_4 = (1.18 \pm 0.16(0.10)) \times 10^{-10}$ molecule^{-1} cm^3 s^{-1} [c]							
12.0	303 ± 4	3.4/2.7	1.7/4.7	13.1	44.5	3.29 ± 0.45	1.24 ± 0.36(0.55)
12.0	306 ± 4	5.2/4.1	2.4/6.3	9.3	47.2	4.05 ± 0.66	1.18 ± 0.42(0.52)
11.9[d]	308 ± 4	5.1/5.3	2.4/8.0	11.1	60.0	3.94 ± 0.63	1.11 ± 0.40(0.44)
11.8	305 ± 4	3.2/3.4	1.1/6.4	9.2	25.5	3.61 ± 0.38	1.15 ± 0.17(0.22)
12.0	305 ± 4	3.7/3.3	1.6/6.1	8.1	26.8	3.41 ± 0.36	1.05 ± 0.15(0.18)
12.0	308 ± 4	3.4/2.8	1.4/5.2	6.9	17.2	3.97 ± 0.44	1.27 ± 0.23(0.24)
12.0	306 ± 4	8.2/4.3	2.0/3.7[e]	13.3	18.4	3.75 ± 0.45	1.10 ± 0.14(0.17)
12.0	306 ± 4	8.2/4.4	3.9/7.2	13.3	18.4	3.61 ± 0.50	1.27 ± 0.17(0.20)
6.0	310 ± 4	4.4/3.3	1.8/5.9	7.4	16.8	3.77 ± 0.56	1.21 ± 0.19(0.21)
3.0	313 ± 4	3.9/2.5	1.6/4.4	9.1	27.4	3.47 ± 0.52	1.18 ± 0.19(0.20)
$T = 500$ K, $k_4 = (1.00 \pm 0.08(0.06)) \times 10^{-10}$ molecule^{-1} cm^3 s^{-1} [c]							
12.0	500 ± 4	3.2/3.0	1.3/7.4	2.6	18.8	2.30 ± 0.20	0.97 ± 0.13(0.18)
12.0	500 ± 4	4.6/3.7	1.9/8.6	3.7	12.6	2.32 ± 0.23	1.06 ± 0.13(0.17)
12.0	500 ± 4	4.6/3.8	1.1/4.9[e]	3.7	12.6	2.46 ± 0.20	0.97 ± 0.10(0.13)
12.0	500 ± 4	8.3[g]/ 4.5	0.8/5.7[e]	6.1	45.4	2.59 ± 0.25	0.93 ± 0.13(0.19)
12.0	500 ± 4	8.3[g]/ 4.5	1.4/10.8	6.1	45.4	2.38 ± 0.29	0.95 ± 0.16(0.20)
12.1	500 ± 4	3.8/2.9	1.8/8.0	10.4	41.9	2.65 ± 0.28	1.10 ± 0.15(0.18)
6.0	500 ± 4	6.2/4.5	2.2/8.6	4.9	13.4	2.29 ± 0.23	1.08 ± 0.13(0.16)
3.0	500 ± 4	5.9/2.8	2.1/5.1	6.0	17.8	1.85 ± 0.19	0.97 ± 0.11(0.13)
$T = 900$ K, $k_4 = (6.6 \pm 0.4(0.3)) \times 10^{-11}$ molecule^{-1} cm^3 s^{-1} [c]							
12.0	900 ± 7	8.3/4.7	1.8/7.6[e]	2.1	46.4	0.74 ± 0.05	0.69 ± 0.06(0.08)
12.0	900 ± 7	8.3/4.9	1.0/4.4[f]	2.1	46.4	0.70 ± 0.05	0.62 ± 0.05(0.06)
12.0	900 ± 7	6.0/2.2	2.2/7.4	2.9	37.4	0.54 ± 0.04	0.61 ± 0.04(0.05)
6.0	900 ± 7	6.2/3.4	1.3/5.7[e]	3.5	41.3	0.47 ± 0.04	0.69 ± 0.06(0.08)
6.0	900 ± 7	6.2/3.4	2.4/10.5	3.5	41.3	0.50 ± 0.04	0.65 ± 0.05(0.08)
3.0	900 ± 7	3.5/2.0	1.2/5.8	6.9	45.6	0.36 ± 0.05	0.71 ± 0.06(0.07)

[a] Uncertainties consist of estimated systematic and 1σ statistical parts (see text, section VI). [b] Uncertainties given in parentheses are 2σ calculated using the alternative method (see text, section VI) based on the recommendation of ICWM (see ref 25). [c] Average value of k_4 at the corresponding temperature. [d] Uncoated quartz reactor used instead of one coated with boron oxide. [e] Laser attenuated with 1 wire mesh (the laser radiation fluence reduced by a factor of 1.8). [f] Laser attenuated with 2 wire mesh. [g] C_2H_3Br used as a precursor for vinyl radicals instead of C_4H_6O.

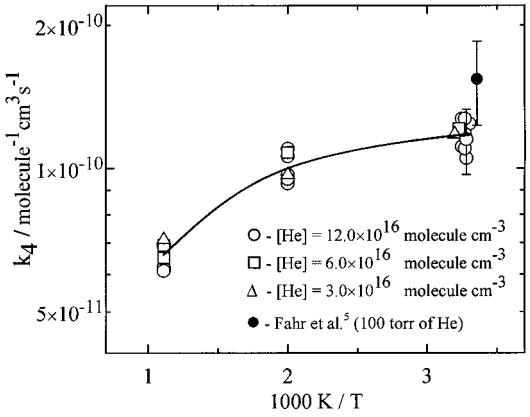

Figure 3. $C_2H_3 + CH_3$ overall rate constants vs 1000 K/T. Current study: open circles, [He] = 12.0×10^{16} molecules cm^{-3}; squares, [He] = 6.0×10^{16} molecules cm^{-3}; triangles, [He] = 3.0×10^{16} molecules cm^{-3}. Uncertainties (see Table 1) are not shown on the plot (except for one point) to avoid congestion. Solid line represents fitting of the experimental results with formula IV (no pressure dependence is assumed). Filled circle, result of Fahr et al.[5] (obtained at room temperature and 13.3 kPa (100 Torr) of He).

are the only important channels of consumption of allyl radicals under the experimental conditions used.

At the highest temperature of the current experiments, 900 K, the reaction of H atom produced in reaction channel 4b with acetone can become sufficiently fast ($k \approx 9 \times 10^{-13}$ molecule^{-1} cm^3 s^{-1}, k[$CH_3C(O)CH_3$] $\leq$ 44 s^{-1} [28]) to occur on the experimental time scale. This reaction produces H_2 and $CH_2C(O)CH_3$ radical, which is expected to immediately decompose forming CH_2CO (ketene) and CH_3 radical. These products will have no influence on the results of the rate and product studies. Production of CH_3 in this process will have a negligible effect on the overall CH_3 kinetics due to the very low concentrations of H atoms and high concentrations of CH_3, which is in large excess over C_2H_3 and all products of reaction 4. The influence of ketene on the C_3H_6 signal is eliminated by the use of acetone-*2*-^{13}C in the product study (see above). At lower temperatures, the only potential channel of H-atom decay is heterogeneous loss since reactions with other species are slow due to either low concentrations of these species or low rate constants (e.g., k(H+CH_3)[CH_3] < 8 s^{-1} [29]).

To establish that the temporal behavior of the product signals is that expected of the primary products of the corresponding reactions, fitting of the room-temperature signals with a simple kinetic model including reactions 4−9 was performed. The overall rate constants for reactions 4 and 5 were taken from the measurements described in section IV. The knowledge of the branching ratios of channels 4a, 4b, and 4c is not necessary to model the shapes of the product signals. The rate constant of the reaction between allyl and methyl radicals (k_8) has been determined by Garland and Bayes[18] to be $(6.5 \pm 2.0) \times 10^{-11}$ molecule^{-1} cm^3 s^{-1} (The uncertainty is for 95% confidence limit as reported by the authors.) under conditions (300 K and 0.53 kPa (4 Torr) of He) similar to those used in this experiment. Knowledge of k_8 was needed only for the fitting of the C_3H_5 and C_4H_8 signal profiles. The initial concentrations of C_2H_3 and CH_3 as well as the rate constants of heterogeneous loss of vinyl (k_6), methyl (k_7), and allyl (k_9) radicals were determined in the product analysis experiments in the same way as in the overall rate constant measurements except that a $B/(B + S)$ correction was made to the decomposition ratio of methyl vinyl ketone. Allyl bromide was used as a precursor for C_3H_5 in the

measurement of the rate constant of heterogeneous loss of this radical.

$$C_3H_5Br \xrightarrow{193\ nm} C_3H_5 + Br \qquad (10)$$

The kinetic model was numerically integrated using the Kinal[22] program. k_8 was adjusted within the reported experimental uncertainties in order to reproduce the experimental signal profiles. The solid lines in Figure 4 represent the results of the fitting ($k_8 = 7.6 \times 10^{-11}$ molecule^{-1} cm^3 s^{-1}). The model is in good agreement with the experimentally obtained signals, supporting the above mechanism of product formation.

Additional room temperature ($T = 306$ K, [He] $= 12 \times 10^{16}$ molecules cm^{-3}) product identification experiments were performed using acetone-d_6 ($CD_3C(O)CD_3$), which produces deuterated methyl radicals (CD_3) as a result of the photolysis. $C_3H_3D_3$, $C_3H_3D_2$, and C_2H_2 were detected as products of the $C_2H_3 + CD_3$ reaction in this system.

Quantitative Determination of Products. *Procedure*. To measure the quantitative yields of the observed products, a calibration had to be performed that related the signal amplitudes to the actual concentrations of the species produced in the system. For the stable products (for example, C_2H_2) such calibration could be performed (vide infra). For allyl radicals, however, a calibration could not be obtained due to the lack of a quantitatively controlled source of these radicals. Instead, the yields of the secondary product, C_4H_8 (assumed to be 1-butene formed as a result of the reaction between allyl and methyl radicals), were measured. It was further assumed that 1-C_4H_8 is the only product of reaction 8. According to the kinetic model used (reactions 4−9) the only two pathways of consumption of allyl radicals are reaction 8 and reaction 9 (heterogeneous loss). Thus, once the yield of 1-C_4H_8 and k_9 are measured, the yield of allyl radicals can be determined provided that k_8 is known.

Another important assumption that was made in the quantitative analysis is that the observed C_3H_6 product is propene rather than cyclopropane. The two molecules have very similar ionization potentials and would be virtually indistinguishable by the PIMS detection method. This assumption is based on the analysis of kinetic and thermodynamic data available in the literature and the results of high level quantum chemistry calculations performed on this system.[23]

Product signals were measured relative to the ion signal of methyl vinyl ketone in order to compensate for the decay of the intensity of the resonance ionization lamp due to the contamination of the lamp window surface and/or formation of color centers in the window crystals which absorb the UV light. Typically, the lamp intensity decreased by a factor of 1.5−2.0 during the time necessary for accumulation of one product signal (2000−3000 repetitions of experiment, 500−750 s). Product signals were therefore accumulated in a series of short sets of experiments, about 100 repetitions (25 s) each, with the methyl vinyl ketone reference signal recorded before and after each set. The ratio of the product signal amplitude to the $C_2H_3C(O)CH_3$ signal (SigR) did not depend on the lamp intensity and provided a good measure of the product yields. An argon lamp was employed to monitor both C_2H_2 and $C_2H_3C(O)CH_3$ for the acetylene determination. A hydrogen lamp was used to detect C_3H_6, 1-C_4H_8, and methyl vinyl ketone for the propene and 1-butene measurements.

The relative calibration was performed by the simultaneous introduction of controlled flows of a product reagent (acetylene, propene, or 1-butene) and methyl vinyl ketone into the stream of the carrier gas (He). The relative signal intensities at the corresponding masses were monitored with the photolyzing laser turned off. The signals were corrected for background contributions as above:

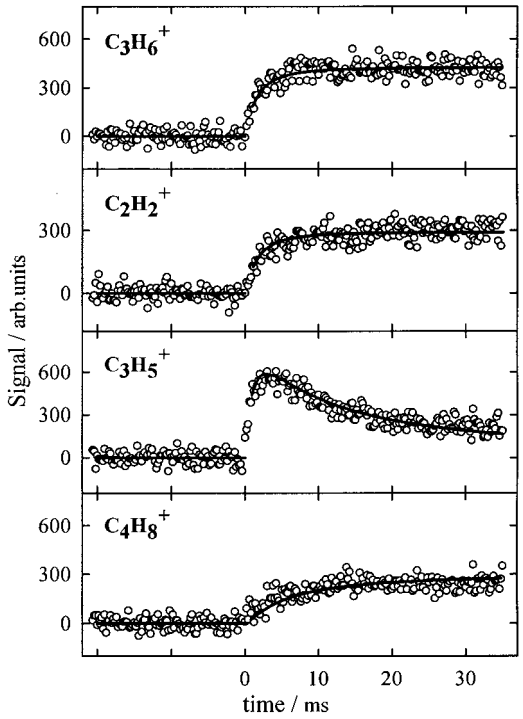

Figure 4. Ion signal profiles of the products of the $C_2H_3 + CH_3$ reaction obtained at 310 K and [He] $= 12 \times 10^{16}$ molecules cm^{-3} ($[C_2H_3]_0 = 2.1 \times 10^{11}$ molecules cm^{-3}, $[CH_3]_0 = 4.8 \times 10^{12}$ molecules cm^{-3}). C_3H_6, C_2H_2, and C_3H_5 are the primary products of the $C_2H_3 + CH_3$ reaction. C_4H_8 is a secondary product (the product of reaction 8). The solid lines represent the results of the fitting of these signal profiles with the kinetic model (see text).

$$\text{signal}_{\text{corrected}} = (\text{signal} - \text{signal}_{\text{scattered light}})\left(1 - \frac{B}{B+S}\right) \qquad (V)$$

The background to background-plus-signal ratios for all the species were determined during each calibration procedure. The calibration yielded the ratios of the sensitivities of the products to that of $C_2H_3C(O)CH_3$ (SenR):

$$\text{SenR} = \frac{\text{signal}_{\text{corrected}}(\text{product})}{\text{signal}_{\text{corrected}}(C_2H_3C(O)CH_3)} \frac{[C_2H_3C(O)CH_3]}{[\text{product}]} \qquad (VI)$$

These sensitivity ratios were then used to calculate the ratios of the product concentrations to the amount of precursor decomposed in the photolysis (PPR):

$$\text{PPR} = \frac{\text{SigR}}{\text{SenR} \times \text{DR}(C_2H_3C(O)CH_3)} \qquad (VII)$$

Product yields were determined after correcting the PPR values for the heterogeneous loss of vinyl radicals using the simple kinetic model consisting of reactions 4−7. Such corrections were minor. Typically, 5−10% of all vinyl radicals formed as a result of photolysis were not available for reaction with CH_3 due to the heterogeneous loss.

Ancillary experiments were conducted to determine the products of the heterogeneous reactions of C_2H_3 and CH_3 using low initial concentrations of these radicals to avoid any influence of recombination. No products could be detected because of a combination of insufficient sensitivity and the fact that, wall-

TABLE 2: Experimental Conditions and Product Yields Obtained in the Study of the $C_2H_3 + CH_3$ Reaction

10^{-16}[He], molecules cm^{-3}	10^{-11}[C_4H_6O]/10^{-13}[C_3H_6O], molecule cm^{-3}	10^{-11}[C_2H_3]$_0$/10^{-12}[CH_3]$_0$, molecule cm^{-3}	product yields,[a] %				bal,[d] %
			C_3H_6	C_2H_2	C_4H_8[b]	C_3H_5[c]	
		$T = 310 \pm 4$ K					
3.0	4.7/2.7	2.5/5.8	41 ± 5(5)	32 ± 9(10)	19 ± 3(3)	25 ± 5(5)	98
12.0	6.4/4.2	2.6/6.5	46 ± 7(8)	45 ± 8(8)	12 ± 2(2)	15 ± 3(3)	106
12.0	7.2/4.3	2.1/4.8[e]	39 ± 12(12)	44 ± 12(12)	11 ± 2(2)	14 ± 3(3)	97
		$T = 500 \pm 4$ K					
3.0	5.8/2.8	2.6/6.5	27 ± 5(5)	49 ± 9(10)	25 ± 4(4)	28 ± 5(5)	104
12.0	6.1/3.0	2.4/5.8	32 ± 5(5)	52 ± 12(12)	13 ± 2(2)	15 ± 3(3)	99
		$T = 900 \pm 7$ K					
3.0	6.2/1.9	3.1/6.0	9 ± 7(8)	29 ± 5(5)	57 ± 6(6)	59 ± 8(8)	97
12.0	5.1/1.6	2.4/5.0	16 ± 8(8)	27 ± 6(6)	47 ± 5(5)	50 ± 8(8)	93

[a] Uncertainties consist of estimated systematic and 1σ statistical parts (see text, section VI). Uncertainties given in parentheses are 2σ calculated using the alternative method based on the recommendation of ICWM (see ref 25). [b] Product of the $C_3H_5 + CH_3$ secondary reaction. [c] Determined from C_4H_8 yield (see text, section V). [d] Product balance. [e] Laser attenuated with 1 wire mesh (the laser radiation fluence reduced by a factor of 1.5).

loss processes having relatively low rates, only a fraction of radicals decayed on the walls in these experiments.

The product ion signal determinations were affected by the presence of minor background signals at the masses of the products under study (C_2H_2, C_3H_6, and C_4H_8). The signals originated from the photolysis of acetone-2-^{13}C and/or its impurities. At each relevant mass, the value of the background signal was determined by measuring the signal amplitude at the mass of the corresponding product with only $CH_3{}^{13}C(O)CH_3$ and He bath gas present in the system and with approximately the same average resonance lamp intensity as that used to monitor the corresponding product. The values of the background were usually 5−20% of the corresponding product signal amplitudes and were subtracted from the product signals prior to the product yield calculations.

The quantitative product analysis experiments performed under each set of experimental conditions (T, [He], and [CH_3]$_0$/[C_2H_3]$_0$) consisted of the following sequence of measurements:

1. Kinetics of heterogeneous loss of C_2H_3 (determination of k_6).
2. Kinetics of heterogeneous loss of CH_3 (determination of k_7).
3. Decomposition ratios of $C_2H_3C(O)CH_3$ and $CH_3{}^{13}C(O)CH_3$ (determination of [C_2H_3]$_0$ and [CH_3]$_0$).
4. Kinetics of methyl radicals in the presence of vinyl radicals.
5. Kinetics of vinyl radicals in the presence of methyl radicals.
6. Kinetics of formation of C_3H_6 (relative to $C_2H_3C(O)CH_3$ signal).
7. $CH_3{}^{13}C(O)CH_3$ background signal at the mass of C_3H_6.
8. Kinetics of formation of C_4H_8 (relative to $C_2H_3C(O)CH_3$ signal).
9. $CH_3{}^{13}C(O)CH_3$ background signal at the mass of C_4H_8.
10. Kinetics of formation of C_2H_2 (relative to $C_2H_3C(O)CH_3$ signal).
11. $CH_3{}^{13}C(O)CH_3$ background signal at the mass of C_2H_2.
12. Kinetics of heterogeneous loss of C_3H_5 (determination of k_9).

The relative calibration was performed after each set of the measurements, during the same experiment. The values of sensitivity ratios (SenR) were stable from experiment to experiment and did not depend on the experimental conditions. A slight increase in SenR(C_2H_2) with increase of temperature was observed.

At 900 K, a substantial ion fragmentation signal from C_3H_5-Br at the mass of allyl radical made it impossible to monitor the C_3H_5 wall-loss kinetics using this precursor. The problem was overcome by using 1,5-hexadiene instead of allyl bromide as the photolytic precursor of C_3H_5:

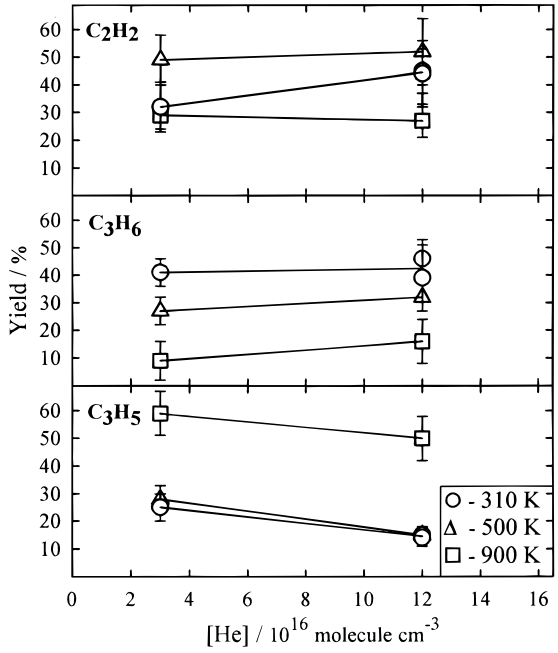

Figure 5. Experimentally obtained product yields of primary products of the $C_2H_3 + CH_3$ reaction (C_2H_2, C_3H_6, and C_3H_5) vs helium bath gas density. Circles, $T = 310$ K; triangles, $T = 500$ K; squares, $T = 900$ K.

$$CH_2CH(CH_2)_2CHCH_2 \xrightarrow{193\ nm} 2C_3H_5 \qquad (11)$$

The measured values of k_9 varied in the product analysis experiments within the range of 7−20 s^{-1} depending on the reactor wall conditions.

Results. The conditions and results of the quantitative product analysis are given in Table 2. The pressure dependence of the product yields is plotted in Figure 5. The yields of C_3H_6, C_2H_2, and C_4H_8 were obtained directly from the corresponding signal amplitudes. The yields of C_3H_5 were obtained from the yields of C_4H_8 with correction for the heterogeneous loss of allyl radicals using kinetic modeling (see above). The only information necessary for the computation of this correction that was not measured in the current experiments was the value of k_8. In the data analysis it was assumed that k_8 does not depend on pressure or temperature and equals 6.5×10^{-11} molecule^{-1} cm^3 s^{-1} (the value determined by Garland and Bayes[18] at 300 K and 0.53 kPa (4 Torr) of He). The assumption is reasonable

taking into account that reaction 8 is similar to the reaction under study and would probably experience a weak negative temperature dependence with no pressure dependence within the range of experimental conditions used in the current work. Although the lack of reliable values for k_8 introduces an uncertainty into the correction, the absolute value of the correction is small. Most of the allyl radicals react with methyl radicals rather than decay on the wall. As a result, the uncertainty in the value of the correction has little impact on the accuracy of the determination of the yields of C_3H_5.

For all experimental conditions, an excellent overall product balance was obtained (see Table 2). The fact that all the vinyl radicals can be accounted for serves as an additional indication of the validity of the experimental approach. The product balance also indicates that no significant products of the $C_2H_3 + CH_3$ reaction have been overlooked in these experiments.

VI. Estimation of Experimental Uncertainties

The sources of error in the measured experimental parameters such as temperature, pressure, flow rate, signal count, and zero time were subdivided into statistical and systematic. Statistical uncertainties were estimated for parameters statistical in the physical nature (for example, signal count) and for parameters for which a series of independent measurements could be performed (for example, flow rate). Statistical uncertainties were taken to be $\pm 1\sigma$. The estimate of possible systematic errors was based on the finite accuracy of the equipment. In cases where the change in the value of the measured parameter (for example, the rate of heterogeneous loss of a radical) during the time of the experiment was significantly larger than the estimated statistical uncertainties of this parameter, the possible error in the parameter was considered to be systematic and taken to be $\pm 1/2$ the difference between the highest and the lowest mean values. In the experimental measurements of product yields, the major source of uncertainty was the presence of a background signal coming from the products of the photolysis of acetone-*2*-^{13}C and/or its impurities at the masses of the detected products. The uncertainty of the background signal was taken to be $\pm 100\%$ of its value and considered to be systematic.

The uncertainties of the measured experimental parameters were propagated to the final values of the rate constants and product yields using different mathematical procedures for propagating systematic and statistical uncertainties.[24] Thus, the error limits of the experimentally obtained values reported in this work (see Tables 1 and 2) represent a sum of 1σ statistical uncertainty and estimated systematic uncertainty.

An alternative method of combining the systematic and statistical parts of the overall uncertainty is that recommended by the NIST policy on reporting uncertainties which, in turn, is based on the recommendation of the International Committee of Weights and Measures (CIPM).[25] This alternative method was also used in the current work. In this approach, the systematic part of the uncertainty was treated as "absolute" (i.e., assuming a rectangular distribution).[25] Corresponding values of 1σ were obtained by dividing absolute uncertainty values by $\sqrt{3}$. Overall uncertainty values (combined standard uncertainty)[25] were obtained by combining the systematic and statistical parts according to the root-sum-of-squares rule. The results of this alternative method of estimating uncertainties are reported as 2σ in parentheses in Tables 1 and 2 and throughout the text. The differences between the results of the two methods of uncertainty estimation are negligible for the product yields and more pronounced for the overall rate constants.

VII. Discussion

The current work is the first direct determination of the rate constant and branching ratios of the $C_2H_3 + CH_3$ reaction performed over a wide range of temperatures and pressures. In Figure 5 it can be seen that the C_2H_2 yields do not experience any pressure dependence (within the experimental uncertainties) at all three temperatures studied. The yields of C_3H_5 decrease with an increase of pressure (the decrease is well resolved at 310 and 500 K). The expected corresponding increase in the yields of C_3H_6 could not be resolved experimentally. The large relative decrease in the yield of C_3H_5 would correspond to a smaller relative increase in the yields of C_3H_6, one which is within the experimental uncertainties of the C_3H_6 yields.

On the basis of these experimental results the following reaction mechanism is proposed for the reaction of vinyl and methyl radicals:

$$C_2H_3 + CH_3 \rightarrow C_2H_2 + CH_4 \quad (4c)$$

$$C_2H_3 + CH_3 \rightarrow CH_3CHCH_2^* \rightarrow CH_2CHCH_2 + H \quad (4b)$$

$$CH_3CHCH_2^* \xrightarrow{[M]} CH_3CHCH_2 \quad (4a)$$

The reaction has two major routes. One proceeds via a direct abstraction of hydrogen atom from vinyl radical by methyl radical resulting in the formation of acetylene and methane (reaction 4c). The other occurs via the formation of chemically activated propene that can undergo either collisional stabilization (reaction 4a) or further decomposition into allyl radical and hydrogen atom (reaction 4b). The rate constant of the direct abstraction route, k_{4c}, is expected to be pressure independent, whereas the branching ratio of decomposition versus stabilization, k_{4b}/k_{4a}, can be expected to decrease with increase of pressure.

The temperature dependence of the overall rate constant (k_4) is shown in Figure 3 and represented by the modified Arrhenius expression IV (see above). The values of the overall rate constants at room temperature obtained in the current work are somewhat lower than those obtained by Fahr et al.[5] (at room temperature and 13.3 kPa (100 Torr) of He), but the uncertainties of both measurements overlap.

Knowledge of the branching fractions of channels 4a, 4b, and 4c, combined with the knowledge of the overall rate constant, enables the determination of absolute rate constant values of individual channels. Experimental temperature dependencies of the rate constants of the two major routes of the reaction between methyl and vinyl radicals, direct abstraction (k_{4c}) and chemical activation ($k_{4a} + k_{4b}$), specified by the proposed reaction mechanism, are shown in Figure 6. Both k_{4c} and ($k_{4a} + k_{4b}$) experience a weak negative temperature dependence with no observable pressure dependence. The results of the fit of the temperature dependencies with an Arrhenius expression (dashed lines in Figure 6) are given by:

$$k_{4c} = 1.5 \times 10^{-11} \exp(385/T) \quad \text{(VIII)}$$

$$k_{4a} + k_{4b} = 3.3 \times 10^{-11} \exp(236/T) \quad \text{(IX)}$$

The expressions VIII and IX have estimated uncertainties of $\pm 40\%$ and $\pm 25\%$, respectively (derived from the uncertainties of individual values and deviations from the fit). The statistical uncertainties of the fits (2σ) are as follows: $2\sigma(\log(A_{4c})) = 0.36$, $2\sigma(E_{4c}) = 363$ K, $2\sigma(\log(A_{4a} + A_{4b})) = 0.08$, $2\sigma(E_{4c}) = 81$ K (if the rate constant is expressed as $k = A \exp(-E/T)$). These

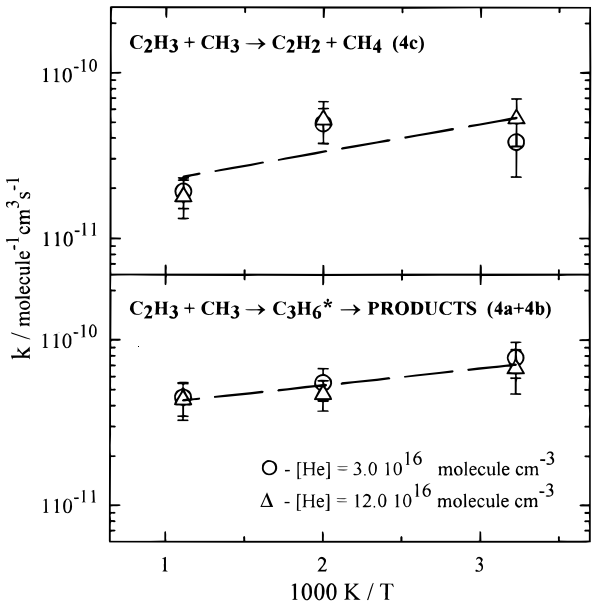

Figure 6. Rate constants of the two major routes of the $C_2H_3 + CH_3$ reaction, direct abstraction, k_{4c}, and chemical activation, $k_{4a} + k_{4b}$, vs 1000 K/T. Circles, [He] = 3.0×10^{16} molecules cm^{-3}; triangles, [He] = 12.0×10^{16} molecules cm^{-3}. The rate constant values are determined from the experimentally obtained overall rate constants and product yields of the corresponding channels. Dashed lines represent the results of fitting of k_{4c} and $k_{4a} + k_{4b}$ temperature dependencies with formulas VIII and IX, respectively (No pressure dependence is assumed.).

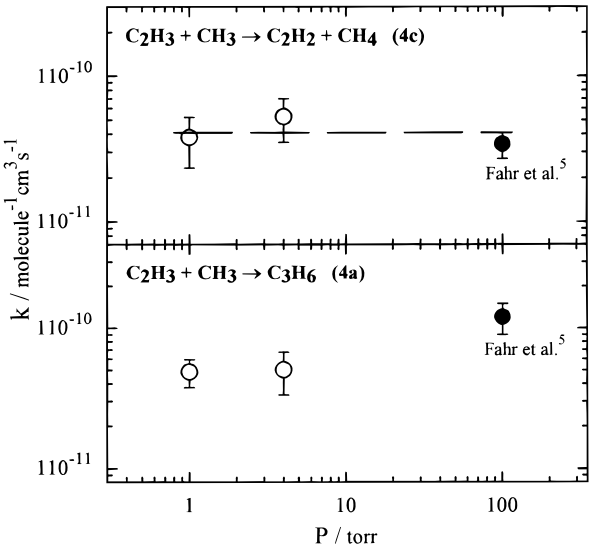

Figure 7. Room temperature rate constants of the channels 4c and 4a vs pressure. Open circles, the results obtained in this work (Rate constants are determined from the experimentally obtained overall rate constants and product yields of the corresponding channels.); filled circles, the results of Fahr et al.[5] The straight horizontal dashed line represents the average value of k_{4c}.

values, however, refer to parametrized fits and have no physical meaning.[27] Although the Arrhenius plot of k_{4c} suggests curvature, experimental uncertainties (which are larger for individual channel rate constants than for the overall reaction due to the additional uncertainties from the experimental values of the branching ratios) do not permit drawing any conclusion about the curvature.

To examine the pressure dependence of the channels 4c and 4a on a larger pressure scale, the room-temperature results of the current experiments and the results of Fahr et al.[5] (obtained at room temperature and 13.3 kPa (100 Torr) of He) were plotted together in Figure 7. Channel 4c still does not show any pressure dependence within the experimental uncertainties whereas k_{4a} increases with the increase of pressure. These trends are in agreement with the proposed reaction mechanism.

The weak negative temperature dependence of the rate constant of the chemical activation route ($k_{4a} + k_{4b}$) is not unexpected. This type of dependence is frequently observed for radical−radical recombination processes.[26] The direct abstraction route (reaction 4c) belongs to the disproportionation type of radical−radical reactions. The data on the temperature dependencies of rate constants of such types of reactions are very sparse. A discussion of the experimentally obtained temperature dependence of k_{4c} in relation to the results of quantum chemistry calculations performed on the $C_2H_3 + CH_3$ potential energy surface will be presented in a forthcoming publication.[23]

Acknowledgment. This research was supported by the Division of Chemical Sciences, Office of Basic Energy Sciences, Office of Energy Research, US Department of Energy under Grant No. DE-FG02-94ER1446. The authors thank Drs. L. J. Stief, R. P. Thorn, Jr., and A. Fahr for helpful discussions.

References and Notes

(1) Tsang, W.; Hampson, R. F. *J. Phys. Chem. Ref. Data* **1986**, *15*, 1087.
(2) Warnatz, J. In *Combustion Chemistry*; Gardiner, W. C., Jr., Ed.; Springer-Verlag: New York, 1984.
(3) Gladstone, G. R.; Allen, M.; Yung, Y. L. *Icarus* **1996**, *119*, 1.
(4) Romani, P. N.; Bishop, J.; Bezard, B.; Atreya, S. *Icarus* **1993**, 106, 442.
(5) Fahr, A.; Laufer, A. H.; Klein, R.; Braun, W. *J. Phys. Chem.* **1991**, *95*, 3218.
(6) Preliminary results were presented at the First Joint Meeting of the U.S. Sections of the Combustion Institute, The George Washington University, Washington, DC, March 1999.
(7) Slagle, I. R.; Gutman, D. *J. Am. Chem. Soc.* **1985**, *107*, 5342.
(8) Slagle, I. R.; Park, J.; Heaven, M. C.; Gutman, D. *J. Am. Chem. Soc.* **1984**, *106*, 4356.
(9) Certain commercial instruments and materials are identified in this article to adequately specify the procedures. In no case does such identification imply recommendation or endorsement by NIST, nor does it imply that the instruments or materials are necessarily the best available for this purpose.
(10) Okabe, H. *Photochemistry of Small Molecules*; Wiley: New York, 1978.
(11) Daly, N. R. *Rev. Sci. Insrum.* **1960**, *31*, 264.
(12) Shoemaker, D. P.; Garland, C. W. *Experiments in Physical Chemistry*; McGraw-Hill: New York, 1962.
(13) Howard, C. J. *J. Phys. Chem.* **1979**, *83*, 3.
(14) Krasnoperov, L. N.; Niiranen, J. T.; Gutman, D.; Melius, C. F.; Allendorf, M. D. *J. Phys. Chem.* **1995**, *99*, 14347.
(15) Lightfoot, P. D.; Kirwan, S. P.; Pilling, M. J. *J. Phys. Chem.* **1988**, *92*, 4938.
(16) Fahr, A.; Braun, W.; Laufer, A. H. *J. Phys. Chem.* **1993**, *97*, 1502.
(17) Niiranen, J. T.; Gutman, D. *J. Phys. Chem.* **1993**, *97*, 9392.
(18) Garland, L. J.; Bayes, K. D. *J. Phys. Chem.* **1990**, *94*, 4941.
(19) Arthur, N. L.; Newitt, P. J. *Can. J. Chem.* **1985**, *63*, 3486.
(20) Slagle, I. R.; Gutman, D.; Davies, J. W.; Pilling, M. J. *J. Phys. Chem.* **1988**, *92*, 2455.
(21) Lias, S. G.; Bartmess, J. E.; Liebman, J. F.; Holmes, J. L.; Levin, R. D.; Mallard, W. G. Gas Phase Ion and Neutral Thermochemistry. *J. Phys. Chem. Ref. Data* **1988**, *17* (Suppl. No. 1).
(22) Turanyi, T. KINAL Version 2.0, Program Package for Kinetic Analysis of Reaction Mechanisms. *Comput. Chem.* **1990**, *14*, 253.
(23) Stoliarov, S. I.; Knyazev, V. D.; Slagle, I. R. Manuscript in preparation.
(24) Bevington, P. R. *Data Reduction and Error Analysis for the Physical Sciences*; McGraw- Hill: New York, 1969.
(25) Taylor, B. N.; Kuyatt, C. E. *Guidelines for Evaluating and Expressing the Uncertainty of* NIST Measurement Results; NIST Technical Note 1297; U.S. Government Printing Office: Washington, DC, 1993.
(26) Heal, M.; Pilling, M. J. In *The Chemical Dynamics and Kinetics of Small Radicals*; Liu, K., Wagner, A., Eds.; World Scientific: Singapore, 1995.

(27) Uncertainties in parameters of the rate constant parametrized expressions have no physical meaning and are reported here at the request of an anonymous reviewer.

(28) Ambidge, P. F.; Bradley, J. N.; Whytock, D. A. *J. Chem. Soc., Faraday Trans. 1* **1976**, *72*, 1870.

(29) Baulch, D. L.; Cobos, C. J.; Cox, R. A.; Esser, C.; Frank, P.; Just, Th.; Kerr, J. A.; Pilling, M. J.; Troe, J.; Walker, R. W.; Warnatz, J. *J. Phys. Chem. Ref. Data* **1992**, *21*, 411.